TABLE I
TERMS TO DERIVE THE S-PARAMETER MODULES FROM THE CHARTS IN FIGS. 3–6

$\|S_{21}\|$
$R_{io} = R_0 + R_{ie}$
$R_{dso} = \frac{R_{dse} R_0}{R_{dse} + R_0}$
$C_{gse}(pF) R_{io} f(GHz)$
$C_{dse}(pF) R_{dso} f(GHz)$
$\|S_{11}\|$
$C_{gse}(pF) f(GHz)$
$\|S_{22}\|$
$C_{gdh}(pF) = C_{gd}(pF)\left(1 + g_m(S) R_0 + \frac{C_{ds}(pF)}{C_{gd}(pF)}\right)$
$R_{dsh} = r_s + r_d + R_{ds}(1 + g_m(S) r_s)$
$C_{gdh}(pF) f(GHz)$
$\|S_{12}\|$
$C_{gsw}(pF) = C_{gd}(pF) R_0 \left(g_m(S) + \frac{1}{R_{ds}}\right) + C_{gs}(pF)\left(1 + \frac{R_0}{R_{ds}}\right) + C_{ds}(pF)$
$C_{gd}(pF) f(GHz)$
$C_{gsw}(pF) f(GHz)$

TABLE II
EXAMPLE OF AMPLIFIER DESIGN

a) FET complete model elements

g_m (S)	C_{gs} (pF)	C_{gd}(pF)	C_{ds} (pF)	R_{ds}(Ω)	R_i(Ω)	r_g(Ω)	r_d(Ω)	r_s(Ω)
0.036	0.246	0.024	0.06	279.7	3.12	6.15	3.06	2.1

b) Design-oriented FET model elements and constant parameters (Table I)

R_{dse} (Ω)	R_{ie} (Ω)	C_{gse} (pF)	C_{dse} (pF)
182.9	11.39	0.31	0.99

C_{gse} (pF) R_{io} (Ω)	C_{dse} (pF) R_{dso} (Ω)	C_{gdh} (pF)	R_{dsh} (Ω)	C_{gsw} (pF)
18.97	3.88	0.127	306	0.4

c) MESFET S-parameters from this method

f (GHz)	|S11|	|S21|	|S12|	|S22|
13	0.757	1.46	0.098	0.597
14	0.745	1.38	0.099	0.591

d) Gains and k (The results for the FET complete model are in brackets)

f (GHz)	G_T (dB)	G_{ma} (dB)	G_{TUmax}(dB)	G(dB)	G_A(dB)	k
13	3.3	10.63	8.9	6.99	5.21	1.033
	(3.77)	(10.96)	(9.01)	(7.1)	(5.27)	(0.99)
14	2.77	9.25	8.16	6.29	4.64	1.126
	(3.3)	(9.42)	(8.26)	(6.39)	(4.7)	(1.07)

edges of the frequency band are shown (arrows in Figs. 3–6 indicate the corresponding values). Finally, in Table II(d), the various gains and stability factor calculated by the S-parameters in Table II(c) are listed.

The stability of the MESFET is assured as reported in Table II(d). A $G_{ma} = 9.25$ dB at 14 GHz is obtained. A two-stage amplifier can theoretically provide a transducer gain of about 18.5 dB in the whole frequency band. The simulation of the circuit using Touchstone shows a gain of 19±0.3 dB. In particular, a gain of 18.7 dB at 14 GHz results, very close to the value predicted by this method.

III. CONCLUSION

A set of new, simple, and accurate expressions for computing FET S-parameters as a function of the circuit elements of the FET complete model has been presented in this paper. The fast calculation of the S-parameter modules by four charts permits straightforward evaluation of the main definitions of FET power gain. The accuracy of this simplified procedure was demonstrated by comparisons with the results from simulation of the FET complete model. This method permits the designer to evaluate the FET performance by using only a pocket calculator.

REFERENCES

[1] G. D. Vendelin, *Design of Amplifiers and Oscillators by the S-Parameter Method.* New York: Wiley, 1982.

[2] C. Paoloni and S. D'Agostino, "An approach to distributed amplifier based on a design-oriented FET model," *IEEE Trans. Microwave Theory Tech.*, vol. 43, pp. 272–277, Feb. 1995.

Dual-Mode Helical Resonators

R. S. Kwok and S. J. Fiedziuszko

***Abstract*—High performance and compact size are the most important criteria in filter-based products for satellite communication systems. Succeeding the superconducting and dielectric resonators, the conventional single-mode helical resonator ranks favorably on its high unloaded-Q per volume. Improvement of the performance has been demonstrated by operating the helical resonator at a higher order $(n > 0)$ mode. In addition, these resonators can also be fabricated onto a high dielectric-constant material to further reduce the size of the filter structure. Detailed design considerations of the dual-mode wire-wound helical resonator filter, as well as implementation of the dual-mode dielectrically loaded helical resonator filter structure, are presented in this paper.**

I. INTRODUCTION

Helical filters have been used extensively in RF and low microwave frequencies in which the conventional lumped-element filters are too lossy and the quarter-wave coaxial resonators are too large. These helices are designed to operate in their cylindrically symmetric fundamental mode $(n = 0)$. Details of such technology have been reviewed by a number of authors [1]–[3]. To further reduce the size of the single-mode helical filters, dielectric-loaded helices have recently been introduced [4]. At the same time, a higher order dual-mode helical filter was also proposed. Design of this higher order helical resonator is very complicated and not yet fully understood, mainly because of the absence of an analytical solution. In this paper, we present the design concept, the approximation used, and the experimental realization of a half-wavelength dual-mode helix loaded cavity filter. Similar to the single-mode resonators, the dual-mode helices can also be fabricated onto a high dielectric-constant material. Results of these newly developed dual-mode dielectric-loaded helical resonators will also be discussed.

Manuscript received October 19, 1998; revised December 10, 1999.

The authors are with Space Systems/LORAL, Palo Alto, CA 94303 USA (e-mail: kwok.raymond@ssd.loral.com).

Publisher Item Identifier S 0018-9480(00)02062-7.

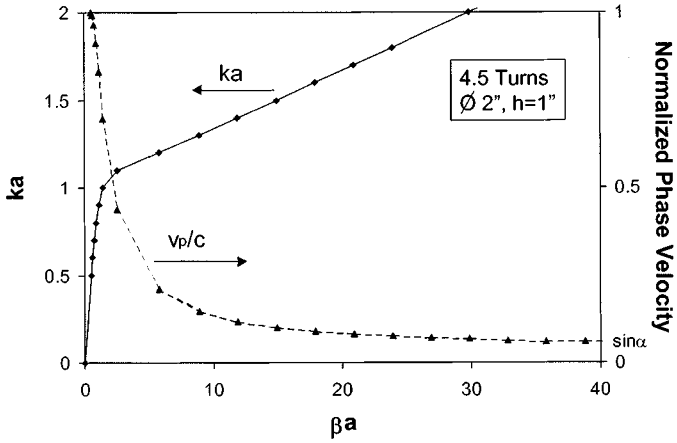

Fig. 1. Dispersion relation and phase velocity of a sheath helix operating at $n = 1$ mode.

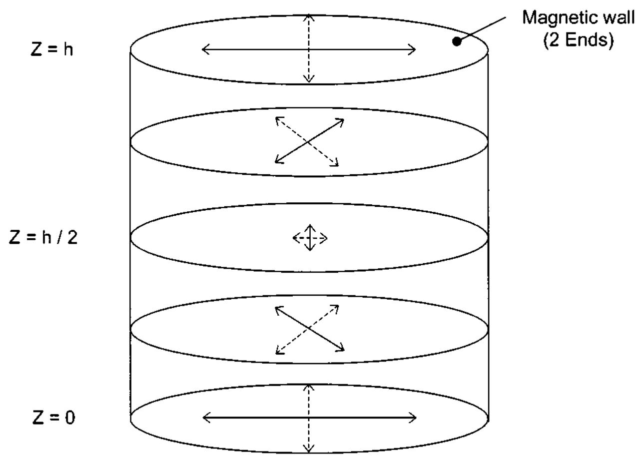

Fig. 2. Oscillating electric-field pattern for the two orthogonal modes of an $n = 1$ half-wave helical resonator.

II. SHEATH MODEL

The sheath model is a popular mathematical description of a helix because of its simplicity and ability to account for many helical properties. A sheath helix is basically a cylindrical tube assumed to have infinite conductivity in the direction of the original helical winding and zero conductivity in a direction normal to the turns of the winding. Excellent literature on the sheath model [5]–[8] are readily available, including a detailed 1995 review by Sensiper.

Following the derivations outlined by Collin [5] and Sensiper [6] for an nth-order sheath helix, one would obtain a transcendental eigenvalue equation

$$\frac{K_n'(ha)I_n'(ha)}{K_n(ha)I_n(ha)} = -\frac{(h^2a^2 + n\beta a \cot\alpha)^2}{K_o^2a^2h^2a^2\cot^2\alpha} \tag{1}$$

where k_o is the free-space phase constant $(=\omega/c)$, β is the axial phase constant $(=\omega/v)$, v is the phase velocity of the wave, h is the radial phase constant defined by $\beta^2 = h^2 + k_o^2$, α is the pitch angle, I_n and K_n are the modified Bessel functions of order n, and the primes are the derivative of the Bessel functions with respect to the argument ha. The guided wavelength can then be approximated by numerically solving this eigenvalue equation. Similar to the dielectric resonator, the lowest order eigenstate of a helical resonator that displays the duality nature

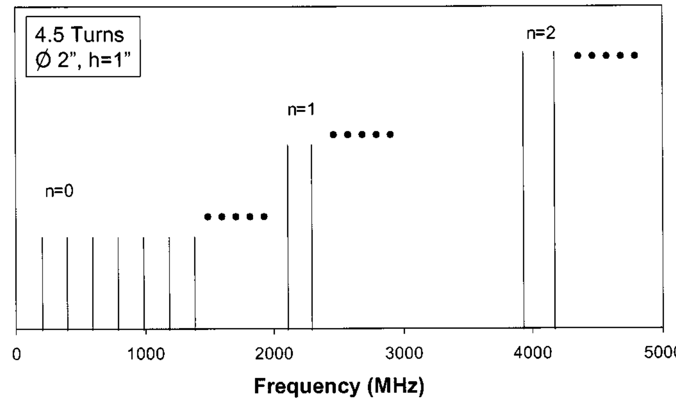

Fig. 3. Spectrum for $n = 0, 1$, and 2 modes of a helical resonator approximated by the sheath model.

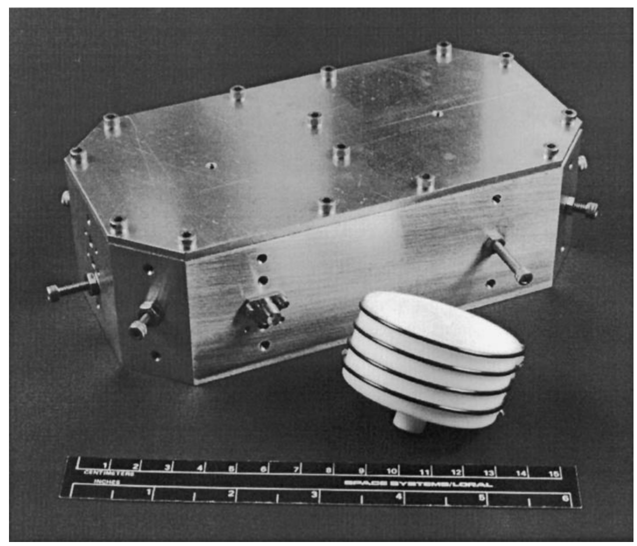

Fig. 4. Dual-mode helical resonator loaded cavity filter (copper helix on Teflon core in bare aluminum cavities).

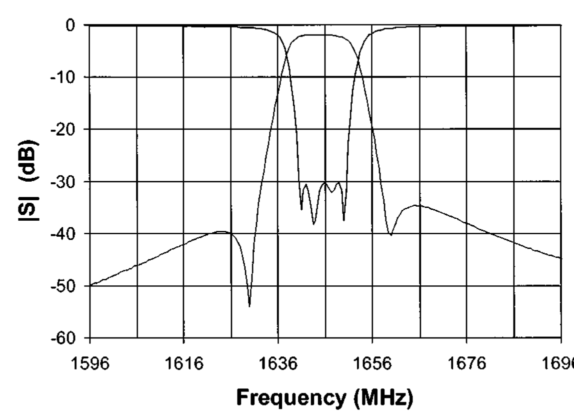

Fig. 5. Measured quasi-elliptical response of a dual-mode helical resonator loaded cavity filter (four pole 10-MHz bandwidth, 1.8-dB insertion loss, realized unloaded Q of 1400).

of the electromagnetic-field pattern is the $n = 1$ mode, even though the field distributions of the two cases are quite different.

For a helix of 4.5 turns, 2-in diameter, and 1-in height, (1) has been solved numerically for the case of $n = 0, 1$, and 2. The resulted dispersion relation and the phase velocity for $n = 1$ mode (shown in Fig. 1)

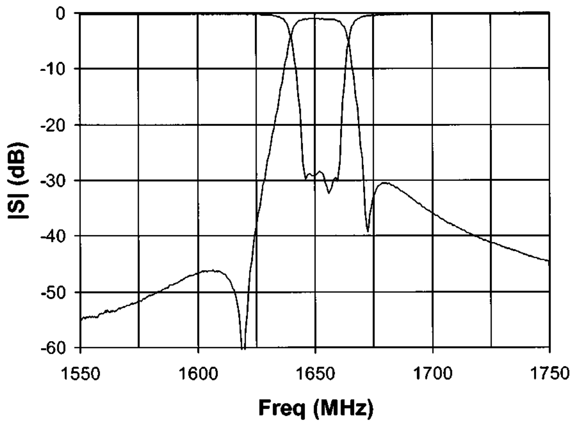

Fig. 6. Measured response of the same filter in Fig. 4 with silver-plated elements and new coupling probes (quasi-elliptical response, 15-MHz bandwidth, 0.96-dB insertion loss, realized unloaded Q of 1800).

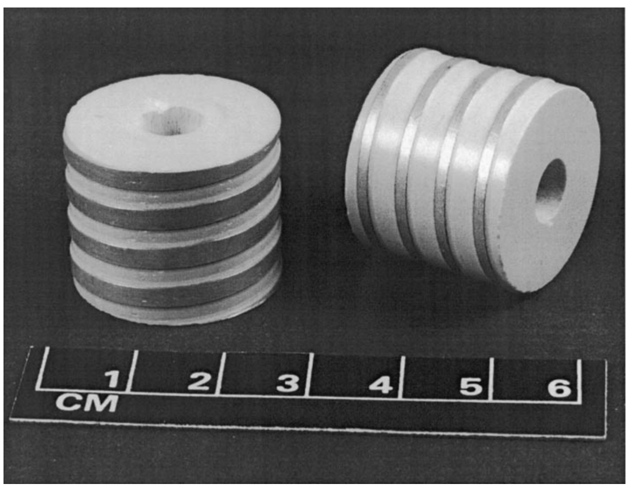

Fig. 7. Helical patterns fabricated onto dielectric resonators of 1-in diameter and 0.8-in height.

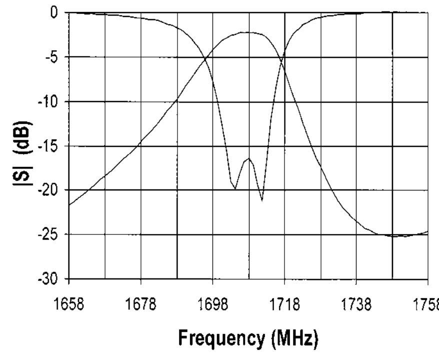

Fig. 8. Measured response of the dual-mode dielectric loaded helical resonator in Fig. 7 (single resonator, 12-MHz bandwidth, 2.2-dB insertion loss, realized unloaded Q of 500).

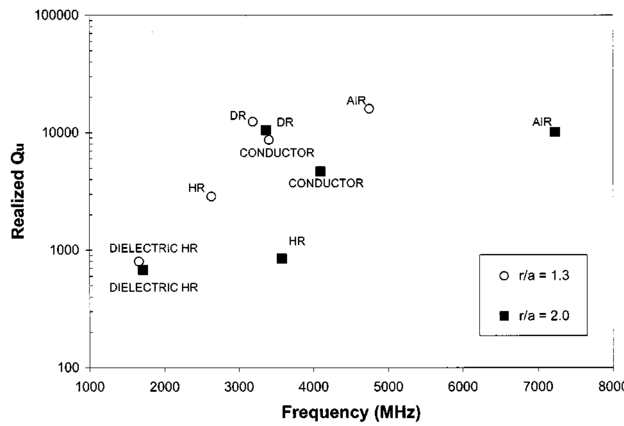

Fig. 9. Realized unloaded Q of the dual-mode cavity resonators with various loading (open circles: $r/a = 1.3$, solid squares: $r/a = 2.0$).

is similar to those of the fundamental mode [5]–[8]. For large $k_o a$, the wave can be thought of as spiraling along the helix and, consequently, the phase velocity is reduced by the geometric factor of $\sin\alpha$.

The corresponding field distributions obtained is similar to that of the HE_{11} hybrid mode of a dielectric resonator with the following noticeable differences.

1) The field intensity is mostly concentrated around the circumference and is minimal at the center.
2) The field direction spiral along the helix.
3) The radial electric field inside and outside of the helix are opposite in direction.

By imposing a reflective boundary at each of the two ends, a spiral standing wave is formed as illustrated in Fig. 2 for the case of using perfect magnetic walls. One can see that two independent sets of solutions exist (solid and dashed lines) in Fig. 2 corresponding to the two orthogonal modes. Depending on how the boundaries are physically implemented, electric walls can also be used provided a 180° phase shift is included upon reflection. Nevertheless, the following discussions apply to either condition.

Finally, spectrum of the nth-order helical resonator mode can be approximated by equating L to an integer multiple of $\lambda_g/2$. The estimated resonant frequencies of the sheath helix for $n = 0$, 1, and 2 modes are shown in Fig. 3. The fundamental spectrum $(n = 0)$ is similar to those recently reported [9], in which the frequency-dependent transverse impedance was explicitly taken into account. Utilizing this result, dual-mode helical resonators were discovered. Cavity filters loaded with such resonators were built and tested. Details of the experiment are described in the following section.

III. Dual-Mode Helical Resonator Loaded Cavity Filters

The helical resonators used for the dual-mode filters (Fig. 4) and its measured response of a four-pole Chebyshev filter was previously reported [4]. The quasi-elliptical response of the modified filter is shown in Fig. 5. The center frequency of the filter is around 1.65 GHz, which is somewhat lower than the 2 GHz estimated from the spectrum in Fig. 3. This is due to the oversimplification of our model, in which neither the loading of the cavity, dielectric holder, and coupling mechanism nor the fringing effects are taken into account. The realized unloaded Q of the filter is measured to be 1400. When silver-plated housing, wire, and tuning screws are used, the realized unloaded Q factor is enhanced to 1800 (see Fig. 6).

Fig. 3 suggests that there are many spurious around the desired frequency, which was observed in a dual-mode resonator. However, with an increased number of resonators, most of the spurious are suppressed. Furthermore, helices with different geometry can be mixed together in a way that the unwanted resonant frequencies of each helix are not co-located. Altogether, the spurious can be managed to an acceptable level.

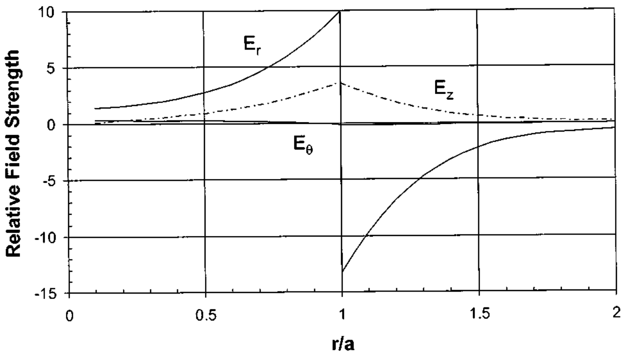

Fig. 10. Maximum strength of the unperturbed electric field components of a $n = 1$-mode sheath helix.

IV. Dual-Mode Dielectric Loaded Helical Resonators

To further reduce the size of the helical resonator, we fabricated helical patterns onto dielectric resonators, as demonstrated in Fig. 7. This can be achieved by using chemical or laser etching, thick silver painting, or electroplating processes. A dielectric resonator of $\varepsilon_r = 20$, 1-in diameter, and 0.8-in height, with four turns of metallic strip was placed inside a cavity of 1.3-in diameter. The first detectable dual-mode resonant is at 1.7 GHz. The realized unloaded Q is about 500–680, as shown in Fig. 8. For a comparison, various types of dual-mode resonators [10]–[13] with the same overall dimensions were measured in the same cavity and the realized unloaded Q are displayed as open circles in Fig. 9. Although this might not be the best way to compare the different technologies because the Q_u is also a function of frequency, it does provide a good reference and is certainly the most economical method. The empty cavity and dielectric resonator loaded cavity have a Q_u of over 10 000. The conductor-loaded cavity is about half of that, and for a four-turn wire-wound helix of 1-in inside diameter, a Q_u of 850 is obtained, which is much too low for that frequency.

In reviewing the electric-field intensity of the sheath model (Fig. 10), we realized that the first filter built has a r/a ratio of 1.6 and a Q_u of 1800. This smaller helix has a ratio of $r/a = 1.3$, where the unperturbed electric field is still quite substantial and, consequently, the Q_u is much lower $(=850)$. Fig. 10 then implied that the cavity should be chosen such that r/a is almost equal to or greater than two. The above experiment was repeated with a larger cavity of 2-in diameter (denoted as solid squares in Fig. 9). The Q_u of the same wire-wound helix was increased to 2880. Note that both the air cavity and conductor-loaded cavity had improved their Q_u to 16000 and 8700, respectively, while the dielectric resonator and dielectric loaded helix varied only slightly in Q_u and resonant frequency because the electric field is mostly concentrated inside the dielectric. Since the Q_u is not limited by the $\tan\delta$ of the dielectric, one could, in principle, use a higher dielectric constant and a smaller cavity to significantly further reduce the size of the helical resonator.

The Q_u of the resonators reported here are not optimized to their full potential. The realized Q_u is measured by the filter response, which includes all the losses from the structure and coupling mechanisms. With an increased coupling, the measured Q_u can be reduced substantially. The helical resonators under study required very strong coupling, which, in turn, limited the Q_u. Different coupling mechanisms should be investigated to maximize the available Q_u of these filter structures.

V. Conclusion

Novel configurations for dual-mode wire-wound and dielectric loaded helical resonator filters have been demonstrated. Excellent experimental results have been obtained in this initial work and substantial improvement is expected. However, significant theoretical work needs to be completed to explore the full potential of the helix structures.

To include the helical symmetry explicitly in our approximations, a tape model [6], [7] was also considered. A periodic dispersion relation was resulted from this periodicity imposed. Nonetheless, our preliminary study indicated that this model does not offer more critical information than the simpler sheath model. Full-wave analyses of more precise representations are needed to fully understand the observed properties such as the helix-orientation dependence of the measurement. Much of the helical resonator characteristics are still not well understood; this opens a new area for theoretical and experimental investigation of these very promising microwave structures.

Acknowledgment

The authors acknowledge PicoFarad, Anaheim, CA, for providing the dielectric resonators used in these experiments.

References

[1] A. I. Zverev, *Handbook of Filter Synthesis*. New York: Wiley, 1976, ch. 9.
[2] P. Vizmuller, *Filters with Helical and Folded Helical Resonators*. Norwood, MA: Artech House, 1987.
[3] W. W. Macalpine and R. O. Schildknecht, "Coaxial resonators with helical inner conductor," *Proc. IRE*, pp. 2099–2105, 1959.
[4] S. J. Fiedziuszko and R. S. Kwok, "Novel helical resonator filter structures," in *IEEE MTT-S Int. Microwave Symp. Dig.*, Baltimore, MD, 1998, pp. 1323–1326.
[5] R. E. Collin, *Field Theory of Guided Waves*. New York: McGraw-Hill, 1960, pp. 637–640.
[6] S. Sensiper, "Electromagnetic wave propagation on helical structures," *Proc. IRE*, pp. 149–161, 1955.
[7] R. E. Collin, *Foundations of Microwave Engineering*. New York: McGraw-Hill, 1966, pp. 580–585.
[8] J. R. Pierce, *Traveling Wave Tubes*. New York: Van Nostrand, 1950.
[9] J. A. Mezak, "Modeling helical air coils for wireless and RF applications," *R.F. Des.*, pp. 77–79, Jan. 1998.
[10] A. E. Atia and A. E. Williams, "Narrow bandpass waveguide filters," *IEEE Trans. Microwave Theory Tech.*, vol. MTT-20, pp. 258–265, Apr. 1972.
[11] S. J. Fiedziuszko, "Dual mode dielectric resonator loaded cavity filters," *IEEE Trans. Microwave Theory Tech.*, vol. MTT-30, pp. 1311–1316, Sept. 1982.
[12] S. J. Fiedziuszko and J. A. Curtis, "Plural-mode stacked resonator filter including superconductive material resonators," U.S. Patent 5 484 764, Jan. 16, 1996.
[13] C. Wang, K. A. Zaki, and A. E. Atia, "Dual-mode conductor-loaded cavity filters," *IEEE Trans. Microwave Theory Tech.*, vol. 45, pp. 1240–1246, Aug. 1997.